Analytica Chimica Acta 1195 (2022) 339422

Contents lists available at ScienceDirect

Analytica Chimica Acta

journal homepage: www.elsevier.com/locate/aca

Elemental mapping of fluorine by means of molecular laser induced breakdown spectroscopy

Maximilian Weiss *, Zuzana Gajarska , Hans Lohninger , Martina Marchetti-Deschmann , Georg Ramer , Bernhard Lendl , Andreas Limbeck **

Institute of Chemical Technologies and Analytics, TU Wien, Getreidemarkt 9, 1060, Wien, Austria

HIGHLIGHTS

- Sputtering of Cu and spray coating of Ca-acetate, were tested to deposit a molecular forming element on the surface of a fluoropolymer.
- Reduction of laser energy by a factor of 4 without loss in sensitivity (LOD about 160 μg g^{-1}) compared to atomic emission.
- Spatially resolved measurements of fluorine distribution via molecular LIBS possible.

GRAPHICAL ABSTRACT

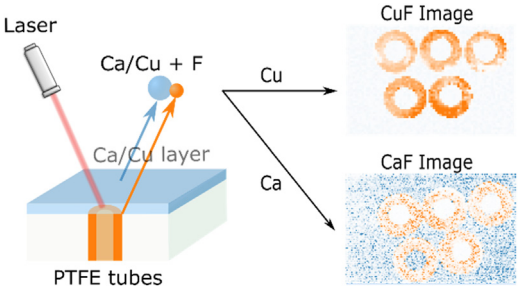

ARTICLE INFO

Article history:
Received 29 October 2021
Received in revised form
21 December 2021
Accepted 30 December 2021
Available online 3 January 2022

Keywords:
Fluorine
Fluoropolymers
Laser induced breakdown spectroscopy
Molecular-LIBS
LIBS imaging

ABSTRACT

The growing importance of fluoropolymers in high-tech applications and green technologies results in the rising need for their characterization. In contrast to conventional methods used for this task, laser-induced breakdown spectroscopy (LIBS) provides the advantage of a spatially resolved analysis. Nevertheless, the high excitation energy of fluorine results in low sensitivity of the atomic F(I) lines, which limits the feasibility of its LIBS-based analysis. This work presents a novel approach for quantitative mapping of fluorine in fluoropolymer samples. It bases on monitoring of molecular emission bands (CuF or CaF) arising from fluorine containing molecules. These species were generated during later stages of the LIBS plasma by a recombination of fluorine atoms originating from fluoropolymer sample with a molecule-forming partner (Cu or Ca) stemming from a surface coating. This approach enables F detection limits in the parts per million (μg g^{-1}) range and elemental imaging using single shot measurements. The elements required for molecular formation are deposited on the sample surface prior to analysis. We evaluate two techniques - spray coating and sputter coating – with regards to their effects on sensitivity and spatial resolution in elemental mapping. Overall, both methods proved to be suitable for a spatially resolved analysis of fluorine: whereas sputter-coating of copper yielded a better sensitivity, spray coating of calcium provided a higher spatial resolution.

1. Introduction

Fluoropolymers are materials with outstanding properties such as mechanical resistance, thermal stability, chemical inertness, and a low dielectric constant [1]. Thus, they have found a myriad of uses

* Corresponding author.
** Corresponding author.
E-mail addresses: maximilian.weiss@tuwien.ac.at (M. Weiss), andreas.limbeck@tuwien.ac.at (A. Limbeck).

https://doi.org/10.1016/j.aca.2021.339422

in different high-tech applications including protective coatings, optical devices, medical implants, insulators and dielectrics or components for automotive industry and aerospace [1–3]. Moreover, fluoropolymers play an important role in the steadily growing field of green technologies [1]. Their annual production reached 320 300 tons in 2018 [4] and is expected to further rise in the future [1].

Nevertheless, the inert nature of these materials results in their low ability to disintegrate over time, which leads to their persistence in the natural environment. Additionally, a recent study suggests possible threat posed by the fluoropolymers related to the release of per- and polyfluoroalkyl substances (PFAS) [4]. Thus, as the production volumes of fluoropolymers rise, the question of their proper disposal becomes of growing concern. Recycling seems to be the best available option, considering the release of hydrogen fluoride and other toxic compounds upon their combustion [5].

As the importance of these materials increases, the need for their characterization steadily grows. The occurrence of fluoropolymers could be assessed with different techniques for analysis of organic macro-molecular compounds or by simple measurement of the element fluorine. State of the art methods for fluorine detection, such as ion chromatography [6], ion sensitive electrodes [7], continuous source atomic absorption spectroscopy (CSAAS) [8] and inductively coupled plasma mass spectrometry (ICP-MS) [9] have in common that they require sample dissolution prior to analysis. For inert materials like fluoropolymers, sample digestion is typically laborious and requires harsh chemicals. Furthermore, it precludes spatially resolved measurements.

We propose to circumvent the dissolution step by using LIBS which has recently gained attention in the field of polymer characterization [10,11]. In contrast to the above-mentioned methods, LIBS is a direct solid sampling technique allowing for a spatially resolved analysis without need for the sample pre-treatment. In LIBS, a short-pulse laser is used to ablate, atomize and excite a small portion of the sample, which results in emission of the characteristic radiation [12]. Its detection results in a complex emission spectrum providing information about the elemental composition of the sample including fluorine.

However, LIBS measurements of fluorine are hindered by the fact that the main emission lines are in the vacuum UV region (below 100 nm) which requires a special instrumental setup. Although additional atomic lines are present in the visible range [13–15], the relatively high excitation energies of the corresponding states [16] require the application of an increased laser energy to achieve a reasonable sensitivity. A possible way to overcome these limitations is the monitoring of molecules containing fluorine. In LIBS, these can arise during later stages of the plasma expansion in which the temperature becomes sufficiently low for the atoms to recombine [17].

The idea of monitoring molecular signals to obtain information about a particular element of interest has been around for a long time [17] and is currently applied in CS-AAS [8] and laser ablation molecular isotopic spectrometry (LAMIS) [18]. In case of LIBS, it was first described for CuCl molecule in 1996 [19] and later applied to the detection of fluorine by means of the CaF emission [20]. Other works dealing with the quantification of fluorine reported an enhancement of the limit of detection (LOD) for fluorine by an order of magnitude when using molecular emissions of CaF [21] and SrF [22] instead of the atomic emission line. Both, the fluorine and the molecular forming elemental partner were either naturally abundant in the sample [14] or the powdered sample was mixed with the element required for molecular formation and pellets were used for measurement [22]. An example of the first approach was the detection of fluorine under Martian conditions [23], the addition of $SrCO_3$ to ore samples to monitor the SrF emission demonstrates applicability of the second methodology [22].

Alvarez-Llamas et al. [16], developed an innovative approach for introducing calcium by liquid nebulization over the sample surface during LIBS analysis. With this approach the analysis of compact samples which do not contain the element required for molecule formation was enabled. In another work, molecular emission was used to quantify fluorine and chlorine in liquid samples by applying them on a calcite substrate [24].

The previously reported methods are well suited for bulk fluorine analysis, nevertheless, they do not allow mapping of the fluorine content. The addition of the molecular forming element as powder is not possible for compact samples and spraying of a liquid is not feasible for water-soluble samples. Moreover, spatially resolved information is so far only reported for samples intrinsically containing both molecular-forming elements [25].

In this work, we present a procedure for the assessment of the fluorine distribution in solid samples using molecular LIBS. Two methods for introducing the molecule-forming partner, enabling the analysis of fluorine in solid materials regardless of their composition, were developed. The first approach is based on sputter deposition of a copper thin film on the sample surface, the second one applies spray deposition of a Ca acetate solution resulting in formation of a thin calcium-acetate layer upon the solvent evaporation. Sputter coating is a widespread method for the deposition of thin films in material sciences [26], however, it has also found application in the field of analytical chemistry. For example prior to SEM-EDX measurements non-conductive samples are coated with a thin layer of elemental carbon [27]. Spray coating is an established method for applying matrices for matrix assisted laser desorption ionization mass spectrometry (MALDI-MS) measurements [28], in particular for imaging applications where a uniform distribution of the MALDI matrix is a prerequisite. The two procedures were employed for the analysis of artificial polymer samples, which enabled identification of their specific benefits and drawbacks.

2. Experimental section

2.1. Preparation of standards

To assess the sensitivity and linearity of the two methods, a series of pressed powder pellets was prepared by combining different amounts of polytetrafluoroethylene (PTFE) powder (particle size 3 μm) from Hagen automation (United Kingdom) with cellulose powder (particle size 20 μm) from Macherey-Nagel (Germany). The weighted powders were premixed with a Vortex Genie 2 shaker (Scientific Industries, USA) and then homogenized in a ball mill (MM 400, Retch Germany) using a shaking frequency of 15 Hz for 2 min. The resulting powder was pressed with a conventional laboratory press (PerkinElmer, Bodenseewerke, Germany). The fluorine content of the prepared standards ranged between 0.6 and 14.5% (w/w). For imaging experiments, five PTFE tubes cut to a length of about 5 mm with an outer diameter of 4 mm and an inner diameter of 2 mm (Bohlender GmbH, Germany) were embedded in a Versocit-2 acrylic resin (Struers, Germany). Prior to analysis, the sample surface was polished using a series of silicon carbide (SiC) grinding papers (Struers, Germany) with grits of 400, 800, 1200, 2000 and 4000. Surface profiles were recorded with a Dektak XT stylus profilometer (Bruker, USA).

2.2. Sputter coating

Copper thin films were deposited via a magnetron sputter coater (Baltech MED-020, Liechtenstein) using a copper target (Micro to Nano, Netherlands) and 150 mA sputter current under

Table 1
Instrumental Parameters used for LIBS measurements.

	Sputtered Cu film	Sprayed Ca layer	F(I) atomic line
Laser energy [mJ]	1.6	1.6	6.5
Spot size [μm]	100	100	100
Frequency [Hz]	10	10	10
Grating grooves [mm^{-1}]	300	300	1800
Stage velocity [mm s^{-1}]	2	1	1
Spot spacing [μm]	200	100	100
Gate delay (ICCD) [μs]	7	2	0.2
Gate width (ICCD) [μs]	10	10	10

0.8 Pa argon atmosphere. After 30 s of pre-sputtering, the actual sputter time was varied between 30 and 200 s.

2.3. Spray coating

Spray coating was performed using a HTX TM Sprayer (HTX Technologies, USA) with a flowrate of 0.03 mL min^{-1}, nozzle temperature of 45 °C, nozzle velocity of 1000 mm s^{-1} and a line spacing of 2 mm. A 37.5 g L^{-1} aqueous solution of calcium acetate, prepared by dissolving calcium acetate (P.A: grade, Merck, Germany) in ultrapure water obtained from a Barnstead EASYPURE II water purification system (Thermo Fisher Scientific, CA, USA), was sprayed onto the sample surface, which resulted in formation of a Ca acetate layer due to the immediate evaporation of the solvent. Multiple application of this spraying procedure on the same sample area enabled optimization of the deposited amount.

2.4. LIBS measurements

LIBS experiments were performed with a J200 Tandem LIBS spectrometer (Applied Spectra Inc., USA), equipped with a 266 nm Nd:YAG laser with 5 ns pulse width and a 6 channel CCD (charge-coupled device) spectrograph covering the spectral range from 188 to 1048 nm. Further an Acton SP2750 spectrometer (Princeton Instruments, USA) with a PIMAX2 1024RB intensified CCD (ICCD) detector (Princeton Instruments, USA) was connected via a fiber bundle to an additional collection optics of the LIBS system. The 6 channel CCD detector was used to monitor broadband emission spectra during imaging experiments, whereas molecular emission and the F(I) atomic emission were recorded with the ICCD system. All measurements were carried out under an argon gas flow of 1 L min^{-1}, except the bulk measurements for atomic emission of fluorine which were performed using a helium flow of 1 L min^{-1} [15]. The parameters used for LIBS measurement are stated in Table 1.

2.5. Data analysis

Raw data was collected with the instrument software (Axiom 2.0 and WinSpec 2.6.24). The data were processed using baseline-corrected integrals [29] The quantitative analysis of the pressed powder standards was performed in OriginPro 2020 (OriginLab Corporation, USA). Graphs were prepared using the python (v 3.7.6, https://www.python.org) programming language and the matplotlib (3.2.3) [30], numpy (1.18.1) [31] and scipy (1.4.1) [32] packages. Images were reconstructed from raw data using Epina ImageLab 3.45 (Epina GmbH, Austria).

3. Results and discussion

3.1. Bulk measurements

In previous molecular LIBS measurements of fluorine [16,22], earth alkali elements were used as molecular forming partners; however, they are too reactive to be sputtered with conventional equipment. Thus, copper was chosen for this work, as it is a rather noble metal frequently applied for magnetron sputtering. Moreover, the CuF molecule emissions in the visible range are free of interference from atomic copper lines [33]. The thickness of the film was optimized in the preliminary experiments to yield the best signal-to-noise ratio. A sputter time of 100 s provided best results and was used for further experiments. This corresponds to a film thickness of 120 nm, measured with a stylus profilometer. Calcium acetate was chosen for spray coating, as calcium was employed in the previous works dealing with the identification of fluorine [16] and acetate as it is a suitable counter-ion introducing no additional elements to polymer samples. Concentration of the calcium acetate and spraying parameters were chosen to provide a nearly continuous layer of calcium acetate, best results were obtained with a mean calcium surface concentration of 0.2 mg cm^{-2}. Details of the molecular bands monitored in the two approaches are described in Table 2.

To assess the sensitivity and linearity of the two methods, pressed powder standards made of cellulose and PTFE were evaluated. PTFE was chosen, as it is the commercially most important fluoropolymer and available in powder as well as in bulk form. These samples were surface treated with both procedures as described before and used for the optimization of LIBS parameters as well as for the assessment of the typical figures of merit. For LIBS analysis, line scans with adjacent single laser shots were performed on an area of 1.2 mm^2 resulting in 60 laser shots for CuF and 120 laser shots for CaF and the measurement of the F(I) atomic line. ICCD gate delays (Table 1) and the wavelength regions (Table 2) used for the analysis were selected in a way to avoid interference from background or prevailing atomic emission lines. To confirm the absence of interfering emissions from trace metals or other constituents of the fluoropolymer LIBS measurements of native PTFE were performed. Using the optimized parameters for gate delay and gate width only weak signals for the C2 swan band were observed, whereas the wavelength regions selected for CuF and CaF

Table 2
Summary of the monitored molecular bands, data from Herzberg. Molecular Spectra and molecular structure-Vol I; [33].

Molecular band	Binding Energy D_0 [eV]	Monitored Transition	v_{00} position [nm]	Spectral region used for integration [nm]
CaF	5.4	$B\ ^2\Sigma^+ \rightarrow X\ ^2\Sigma^+$	530.95	527.13–544.30
CuF	4.4	$C\ ^1\Pi \rightarrow X\ ^1\Sigma^+$	493.36	485.59–498.44

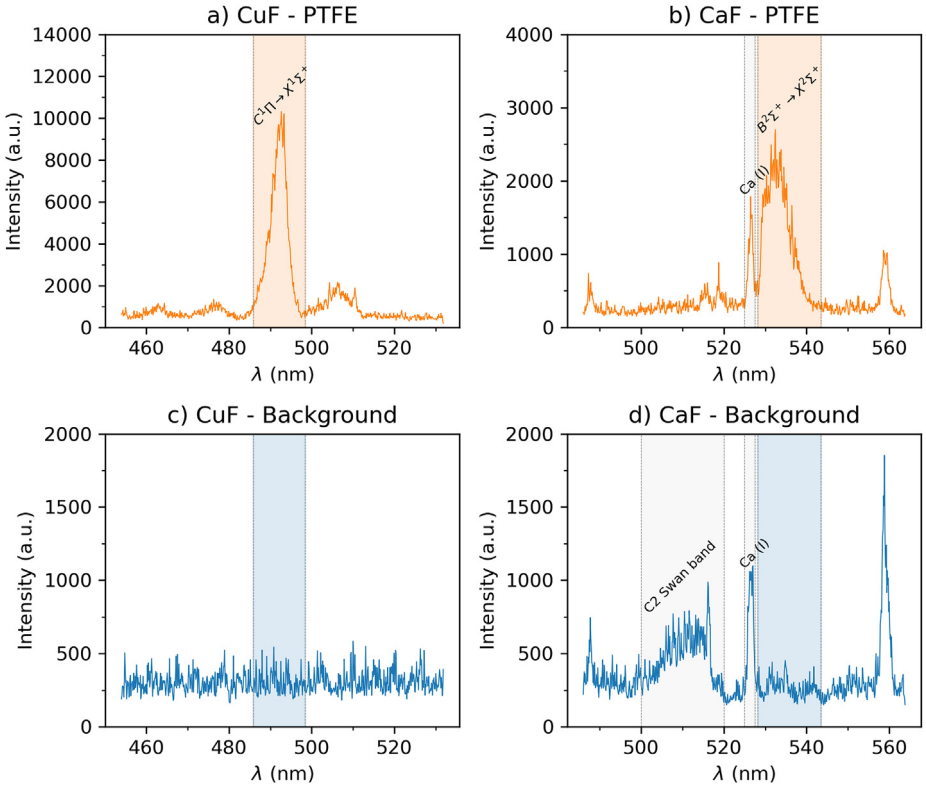

Fig. 1. Single shot spectra of pure PTFE (upper row) and the background acrylic embedding resin (lower row), coated with copper (left) and calcium acetate (right). The areas highlighted in orange/blue indicate the spectral regions integrated and background corrected for image reconstruction, further emission signals from the background acrylic resin are annotated in grey. The exact wavelengths of the used regions are listed in Table 2. (For interpretation of the references to colour in this figure legend, the reader is referred to the Web version of this article.)

measurements showed only signals at the background level. This outcome demonstrates that the molecular emissions obtained in the presence of Cu and Ca are caused exclusively from the generated Fluorine-species (for details see Supplementary Fig. 1). For data evaluation, the spectra were accumulated, and background corrected emission signals were calculated using the spectral regions described in Table 2. For both methods the integrated areas correlated linearly with the fluorine contents of the standards. However, in the case of CaF, the coefficient of determination was not as high ($r^2 = 0.95$) as in the case of CuF ($r^2 = 0.99$). Moreover, the calibration function determined for the CuF approach exhibits a 44 times higher slope, indicating an increased sensitivity for this method. Limits of detection were calculated by dividing three times the standard deviation of the blank by the slope of the calibration curve. This gives fluorine a LOD of 160 μg g^{-1} using CuF and 240 μg g^{-1} using CaF emission, confirming that the CuF approach is more sensitive although less shots were accumulated for CuF than for CaF. A further improvement is possible by increasing the number of shots per measurement, nevertheless achieved findings were in good agreement with literature data, e.g. Alvarez-Llamas et al. [16] report a LOD of 49 μg g^{-1} by averaging the CaF emissions from 140 laser shots for CaF quantification in samples prepared from NaF and Cu powder.

Additionally, the atomic F(I) line at 685.6 nm was investigated to compare the molecule-forming approach to conventional direct detection of atomic lines. For this, a helium atmosphere and the highest possible laser energy of 6.5 mJ was chosen [15]. The standards were analyzed using line scans with adjacent single laser shots with the same 100 μm spacing as used for CaF. As previously, these were accumulated for further analysis. The F(I) atomic line yielded a linear calibration function with an r^2 of 0.94 and an LOD of 160 μg g^{-1}. At first sight, this outcome seems to be comparable with the findings derived for the molecular emissions, however, it must be considered that the applied laser energy was roughly 4 times higher (6.5 mJ for atomic fluorine line vs. 1.6 mJ for the molecular CuF and CaF bands). The substantially higher laser energy necessary for the measurement of atomic lines is a significant drawback. The increased ablation rate reduces the overall in-depth resolution of the method. Additionally, high laser powers restrict the applicability for thermally sensitive samples. On the other hand, measurements with only 1.7 mJ as applied for the CuF and CaF measurements, does not allow for fluorine atomic lines detection.

3.2. Imaging experiments

Bulk measurements normally accumulate multiple measurements taken at different sample locations. For imaging experiments, a so-called continuous scan mode is used [34]. For this, the sample stage moves continuously while the laser is firing repeatedly onto the sample surface. Carefully adjusted repetition rates and scan speeds result in exactly one laser shot per position without overlapping of ablated volumes. Although this measurement mode does not allow signal accumulation, it is the preferred approach for imaging experiments since it enables fast mapping of a rather large area [34]. The suitability of the proposed molecular LIBS procedures for single-shot measurements is very likely but has to be verified. For this purpose, pure PTFE as a representative for a fluorine containing sample and Versocit-2 acrylic resin as an example for a fluorine free sample were analyzed using the conditions reported for bulk measurements, but without the accumulation of individual emission spectra. In Fig. 1, selected regions of single shot spectra acquired from pure PTFE and acrylic resin are

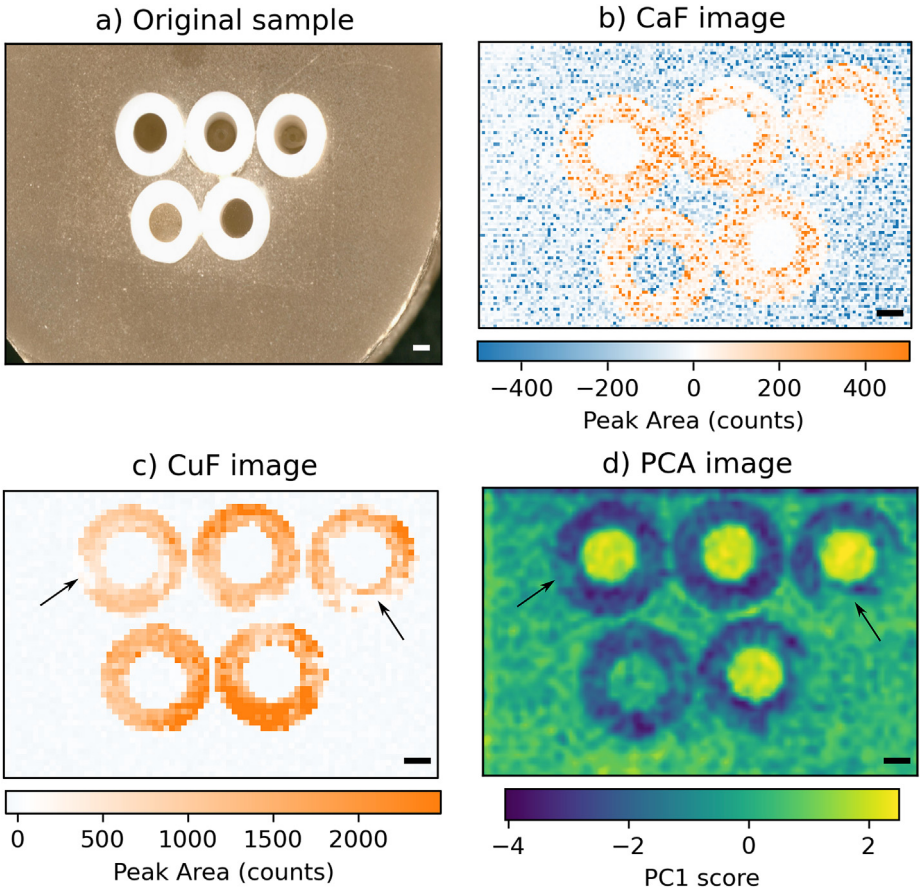

Fig. 2. a: Microscopic image of embedded PTFE tubes used for imaging experiments, b + c: Reconstructed elemental maps from background corrected integrated emission intensities for the (b) CaF, and the (c) CuF molecular band. d: Scores of the first principal component from the broadband six channel detector recorded simultaneously with the molecular CuF band. The scale bar represents 1 mm.

depicted, showing also the areas used for integration of CuF and CaF molecular emissions. It is evident that molecular emissions are measurable even with spectra from single laser shots. Moreover, the significant spectral difference between a blank and the PTFE sample allows simple identification of fluorine containing polymers. This outcome indicates that both coating approaches exhibit sufficient signal intensity allowing ultimately for imaging experiments.

To characterize and compare the mapping capabilities of the two methods, an artificially structured polymer sample consisting of five PTFE tubes embedded in acrylic resin was prepared. The microscopic image of the polished sample is presented in Fig. 2a. Molecular LIBS images of the two samples were acquired by firing single laser shots per sample location using the optimized parameters listed in Table 1. Plotting the intensity of the integrated molecular bands at each acquired position resulted in elemental maps of the CaF (Fig. 2b) and CuF (Fig. 2c) species, which resemble the distribution of fluorine in the sample. Thus, with both techniques, it was possible to reconstruct the PTFE ring structure visible in the microscopic image (Fig. 2a) with a high level of agreement. However, comparing the two coating approaches for the introduction of the molecular-forming partner on the sample surface, distinct differences were observed. At a first glance, the improved sensitivity of the CuF measurement is obvious, which is in agreement with the findings of the bulk investigations reported in the previous section. Besides sufficient sensitivity, spatial resolution is another important parameter for imaging applications. As seen in Fig. 3a, sputter coating results in a continuous film of copper. However, upon laser ablation during the LIBS measurements, the copper layer shows a high tendency to delaminate from the sample. This finding can be attributed to the surface properties of PTFE, which prevent a strong adhesion of the deposited Cu film. Thus, the selected measurement parameters represent a compromise between reasonable signal-to-noise ratio and a fair spatial resolution. In this case, the laser energy of 1.6 mJ per pulse and a laser spot size of 100 μm resulted in the ablation of a circular region of copper exhibiting a diameter of roughly 200 μm. With stylus profilometry it was confirmed that the actual ablation crater still has a size of 100 μm and a depth of about 1 μm. In case of calcium, this behavior was not observed, as the spray coating resulted in separate crystals of calcium acetate on the sample surface (Fig. 3b). However, with LA-ICP-MS measurements it was confirmed that the calcium is present on each part of the sprayed area and not just in the larger crystals (for details see Supplementary Material Fig. 2). Thus, compared to the Cu thin film the sprayed Ca layer is less homogeneous, but offers still a complete surface coverage – a prerequisite for imaging applications. Due to the limitation arising from the delamination of the Cu-film described previously, the CaF image could be acquired with a two times better lateral resolution.

To confirm the applicability of the presented methods for elemental mapping of fluorine, distribution images of PTFE and embedding material were created using the broadband spectra acquired with the 6-channel spectrometer simultaneously to the recording of the molecular bands on the ICCD. To discriminate the PTFE from the embedding materials a set of spectral descriptors representing the baseline-subtracted wavelength ranges of C, H and O atoms, as well as C_2 and CN molecules (see Brunnbauer et al. [35] for a more detailed description of this approach) was

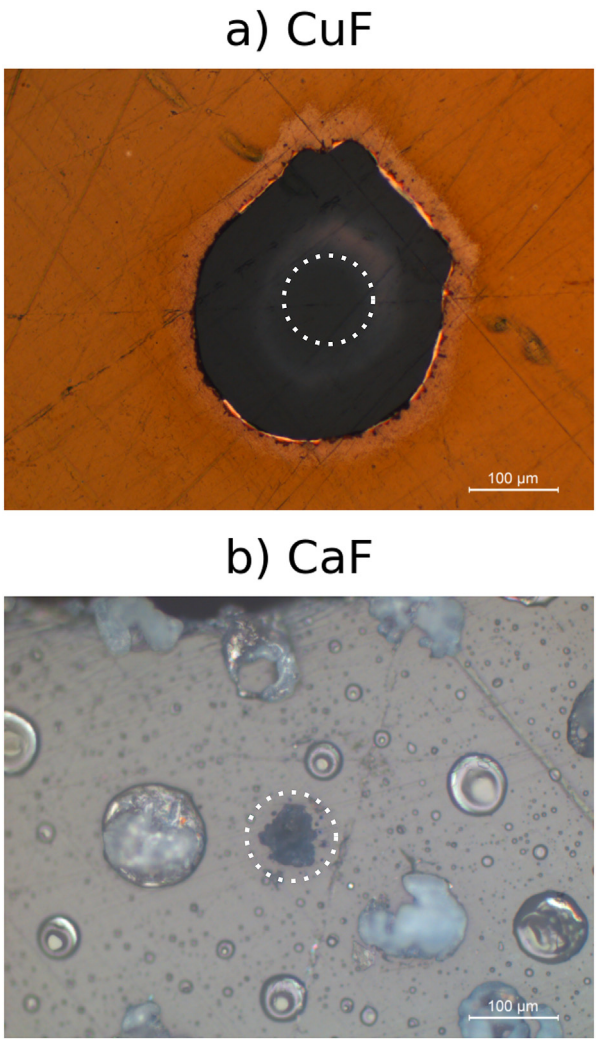

Fig. 3. Detailed view of the crater of one laser shot with 100 µm spot size on (a) copper coated and (b) a calcium acetate sprayed PTFE sample; the marked circle represents the 100 µm laser spot size.

used to extract the polymer-specific information from the raw spectra. An annotated example spectrum with the used spectral descriptors is shown in Fig. 4. The resulting data were subjected to principal component analysis (PCA). Fig. 2d shows the scores of the first principal component, clearly distinguish between PTFE and the embedding material. Compared to the measurement of CuF and CaF molecular emissions this approach offers only limited sensitivity, moreover limited ability to identify and classify fluorine containing polymers in unknown or more complex samples is very likely. Nevertheless, irregularities in the CuF image (Fig. 2c, like in the lower right edge of the third ring - see arrow marks) are also identified by the PCA image (Fig. 2d). As these two images were recorded simultaneously with different collection optics and detection systems, and the failures were observed for the same laser shots (equal to sample positions and thus image-pixels), errors related to signal acquisition are rather unlikely. Instead, sample defects such as artifacts introduced during sample polishing are considered to be responsible for the errors determined in the images.

3.3. Comparison of image quality

To compare the quality of the two fluorine images by advanced data analysis, a mask representing the individual pixels of the PTFE rings and a mask representing the pixels of the background region (acrylic resin) was created for both samples using the microscopic

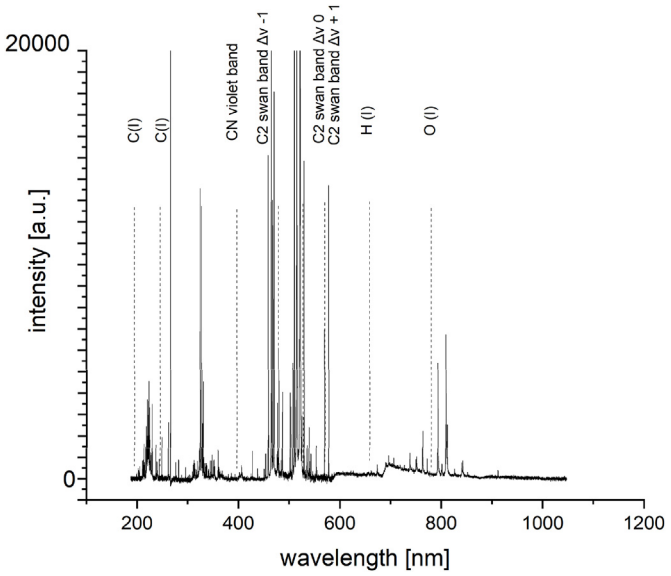

Fig. 4. Exemplary single shot broadband LIBS spectrum recorded with the 6-channel CCD detector during the measurement of the CuF Image in Fig. 2c. The descriptors used to create the PCA image in Fig. 2d are annotated in the spectrum and are taken from Brunnbauer et al., 2020 [35].

image and ImageLab. Using spectral descriptors, the baseline-subtracted molecular bands of CuF and CaF (Table 2) were defined and extracted from the raw spectra. The resulting values were plotted in a histogram representing the distribution of the molecular signal intensities in the region of the PTFE tubes (orange) and the background (blue) for CuF (Fig. 5a) and CaF (Fig. 5b). Furthermore, the means and the variances of the two regions were determined and used for the calculation of Fisher's linear discriminant evaluating the power of discrimination between the two distributions [36,37].

The histograms indicate that using the CuF approach, the signals in the PTFE region can be discriminated from the signals in the background region to a greater extent than in case of the CaF. This observation was confirmed by the Fisher's discriminant values of 2.45 for CuF vs. 0.31 for CaF, whereas a higher value indicates a better discrimination function. Furthermore, a Mann–Whitney *U* test was performed using 300 randomly selected data points (to keep the sample size equal for CuF and CaF) from the ring-PTFE and the acrylic resin, yielding a test statistic of 1687 ($p = 3*10^{-136}$) for CuF and 10 069 ($p = 2*10^{-72}$) for CaF, indicating a highly significant separation of the PTFE from the background for both systems. Thus, the spatial mapping of fluorine in fluoropolymers by means of molecular LIBS proved to be feasible, with sputter coating of copper providing a better discrimination of the fluoropolymer from the background. These numbers confirm the impressions of the elemental maps from Fig. 2, in particular the fluorine mapping obtained using the sputter coating approach seems to offer more homogeneous signal intensities, whereas the spray coating technique delivers signals with higher fluctuations.

To combine the spatially resolved with the statistical information, threshold images of CaF and CuF signal were created (Fig. 5). The threshold was determined with Youden's J statistic [38] and is marked in the associated histograms. With both approaches a classification of the image into fluorine containing and not fluorine containing pixels can be made with a high level of accuracy. However, with CaF the number of misclassified pixels is higher. This outcome could be attributed to the quality of the applied coatings. Copper forms a continuous film on the surface (Fig. 3a), which

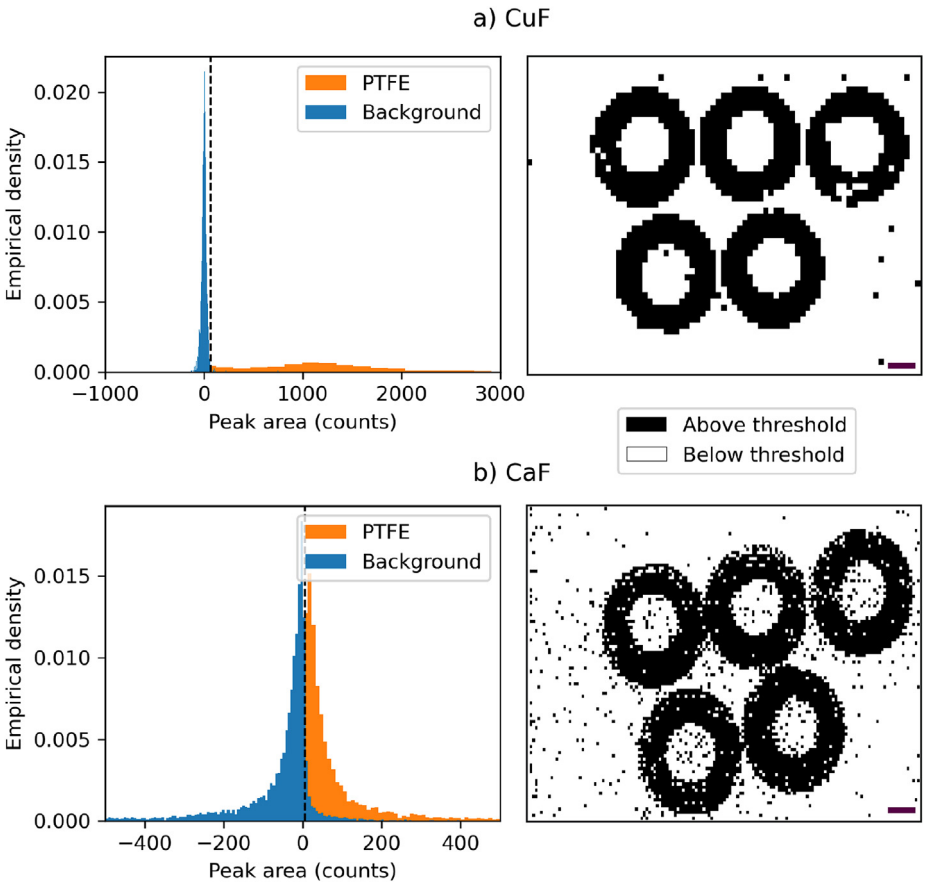

Fig. 5. Left: Histograms representing the distribution of the integrated CuF (a) and CuF (b) molecular band intensities in the region of the PTFE ring (orange) and the acrylic resin (blue). The masks representing the two areas were created using the corresponding optical images. The dotted line represents the PTFE-background threshold determined with Youden's J. Right: Sample images based on the Youden's J threshold. The threshold images of both signals resemble the fluorine distribution present in the optical images. (For interpretation of the references to colour in this figure legend, the reader is referred to the Web version of this article.)

provides constant conditions for the formation of molecules, while the calcium acetate forms stochastically distributed single crystals on the surface of the sample (Fig. 3b), causing distinct point-to-point variations in the emission-intensity of the CaF band.

4. Conclusion

We demonstrated two procedures of applying the element required for molecule formation on a fluorine -containing sample (magnetron sputtering and spray coating), which enabled spatially resolved analysis of fluorine using molecular emission LIBS. Using conventional bulk measurements, the linearity of the analyte content and the measured molecular emission was established and quantitative determination of fluorine in compact solid samples with detection limits in the parts per million ($\mu g\ g^{-1}$) region was shown. Moreover, both methods are sensitive enough to detect fluorine containing molecular emission bands at the single shot level, enabling single shot imaging. Fluorine mappings obtained via measurement of CuF and CaF emission bands were found to be in excellent agreement with the PTFE distribution of the investigated synthetic material, confirming that the proposed molecular LIBS method is able to resemble the fluorine distribution in unknown samples. We used Fisher's linear discriminant as statistical approach to compare the separation power of the signal from the background, yielding that measurement of CuF is better in this aspect, mainly due to the continuous nature of the copper thin film compared to the randomly distributed crystals of the calcium acetate layer. The approach based on magnetron sputtering of a thin Cu film onto the sample surface exhibits further a better linearity in the calibration series and a slightly improved sensitivity. Spray coating of a thin Ca-layer, however, has the advantage of allowing a higher resolution in imaging experiments, as compared to the Cu thin film it does not tend to delaminate during laser irradiation.

To conclude, both methods are feasible for imaging the fluorine distribution in solid samples. Although the present work was focused on measurements of PTFE only, the sensitivity of the two proposed approaches enables also the investigation of other Fluoropolymers with lower fluorine contents. Nevertheless, for a particular application, one must decide whether a higher spatial resolution or a better sensitivity and homogeneity are needed.

Ongoing research will be devoted to improving the adhesion of the Cu thin film and the homogeneity of the Ca layer, enabling further advancements in the spatially resolved analysis of fluorine. Moreover, the proposed coating procedures offer exciting opportunities in combination with molecular LIBS. After appropriate adjustments, analysis of other challenging elements should be possible.

CRediT authorship contribution statement

Maximilian Weiss: Conceptualization, Methodology, Investigation, Formal analysis, Writing – original draft. **Zuzana Gajarska:** Software, Formal analysis, Visualization, Writing – review & editing. **Hans Lohninger:** Software, Resources, Writing – review &

editing. **Martina Marchetti-Deschmann:** Resources, Writing – review & editing. **Georg Ramer:** Software, Formal analysis, Visualization, Writing – review & editing. **Bernhard Lendl:** Resources, Writing – review & editing. **Andreas Limbeck:** Conceptualization, Resources, Project administration, Funding acquisition, Writing – review & editing.

Declaration of competing interest

The authors declare that they have no known competing financial interests or personal relationships that could have appeared to influence the work reported in this paper.

Acknowledgment

This work was supported by the Austrian Science Fund-FWF [grant number P31165-N37]. We want to thank Jakob Willner and Konrad Bielecki for operating the HTX spray coater.

Supporting information

LIBS spectrum of a native PTFE sample, measurement of the homogeneity of the calcium acetate film with LA-ICP-MS, definition and formula for Fisher's linear discriminant and Youden's J.

Appendix A. Supplementary data

Supplementary data to this article can be found online at https://doi.org/10.1016/j.aca.2021.339422.

References

[1] B. Améduri, The promising future of fluoropolymers, Macromol. Chem. Phys. 221 (2020).
[2] H. Teng, Overview of the development of the fluoropolymer industry, Appl. Sci. 2 (2012) 496–512.
[3] J. Lv, Y. Cheng, Fluoropolymers in biomedical applications: state-of-the-art and future perspectives, Chem. Soc. Rev. 50 (2021) 5435–5467, https://doi.org/10.1039/D0CS00258E.
[4] R. Lohmann, I.T. Cousins, J.C. DeWitt, J. Gluge, G. Goldenman, D. Herzke, A.B. Lindstrom, M.F. Miller, C.A. Ng, S. Patton, M. Scheringer, X. Trier, Z. Wang, Are fluoropolymers really of low concern for human and environmental health and separate from other PFAS? Environ. Sci. Technol. 54 (2020) 12820–12828.
[5] S. Ebnesajjad, 13 - safety, disposal, and recycling of fluoropolymers, in: S. Ebnesajjad (Ed.), Introduction to Fluoropolymers, William Andrew Publishing, Oxford, 2013, pp. 293–309.
[6] Y. Noguchi, L. Zhang, T. Maruta, T. Yamane, N. Kiba, Simultaneous determination of fluorine, chlorine and bromine in cement with ion chromatography after pyrolysis, Anal. Chim. Acta 640 (2009) 106–109.
[7] P.A. Mello, J.S. Barin, F.A. Duarte, C.A. Bizzi, L.O. Diehl, E.I. Muller, E.M.M. Flores, Analytical methods for the determination of halogens in bioanalytical sciences: a review, Anal. Bioanal. Chem. 405 (2013) 7615–7642.
[8] S. Mores, G.C. Monteiro, S. Santos Fda, E. Carasek, B. Welz, Determination of fluorine in tea using high-resolution molecular absorption spectrometry with electrothermal vaporization of the calcium mono-fluoride CaF, Talanta 85 (2011) 2681–2685.
[9] W. Guo, L. Jin, S. Hu, Q. Guo, Method development for the determination of total fluorine in foods by Tandem inductively coupled plasma mass spectrometry with a mass-shift strategy, J. Agric. Food Chem. 65 (2017) 3406–3412.
[10] V.C. Costa, F.W.B. Aquino, C.M. Paranhos, E.R. Pereira-Filho, Identification and classification of polymer e-waste using laser-induced breakdown spectroscopy (LIBS) and chemometric tools, Polym. Test. 59 (2017) 390–395.
[11] K. Liu, D. Tian, C. Li, Y. Li, G. Yang, Y. Ding, A review of laser-induced breakdown spectroscopy for plastic analysis, TrAC Trends Anal. Chem. (Reference Ed.) 110 (2019) 327–334.
[12] R.E. Russo, X. Mao, J.J. Gonzalez, V. Zorba, J. Yoo, Laser ablation in analytical chemistry, Anal. Chem. 85 (2013) 6162–6177.
[13] M.A. Gondal, Y.W. Maganda, M.A. Dastageer, F.F. Al Adel, A.A. Naqvi, T.F. Qahtan, Detection of the level of fluoride in the commercially available toothpaste using laser induced breakdown spectroscopy with the marker atomic transition line of neutral fluorine at 731, 1nm, Opt. Laser Technol. 57 (2014) 32–38.
[14] P. Pořízka, S. Kaski, A. Hrdlička, P. Modlitbová, L. Sládková, H. Häkkänen, D. Prochazka, J. Novotný, P. Gadas, L. Čelko, K. Novotný, J. Kaiser, Detection of fluorine using laser-induced breakdown spectroscopy and Raman spectroscopy, J. Anal. At. Spectrom. 32 (2017) 1966–1974.
[15] C.D. Quarles, J.J. Gonzalez, L.J. East, J.H. Yoo, M. Morey, R.E. Russo, Fluorine analysis using laser induced breakdown spectroscopy (LIBS), J. Anal. At. Spectrom. (2014) 29.
[16] C. Alvarez-Llamas, J. Pisonero, N. Bordel, A novel approach for quantitative LIBS fluorine analysis using CaF emission in calcium-free samples, J. Anal. At. Spectrom. 32 (2017) 162–166.
[17] A. De Giacomo, J. Hermann, Laser-induced plasma emission: from atomic to molecular spectra, J. Phys. D Appl. Phys. 50 (2017) 183002.
[18] R.E. Russo, A.A. Bol'shakov, X. Mao, C.P. McKay, D.L. Perry, O. Sorkhabi, Laser ablation molecular isotopic spectrometry, Spectrochim. Acta, Part B 66 (2011) 99–104.
[19] C. Haisch, R. Niessner, O.I. Matveev, U. Panne, N. Omenetto, Element-specific determination of chlorine in gases by Laser-Induced-Breakdown-Spectroscopy (LIBS), Anal. Bioanal. Chem. 356 (1996) 21–26.
[20] M. Gaft, L. Nagli, N. Eliezer, Y. Groisman, O. Forni, Elemental analysis of halogens using molecular emission by laser-induced breakdown spectroscopy in air, Spectrochim. Acta, Part B 98 (2014) 39–47.
[21] C. Alvarez-Llamas, J. Pisonero, N. Bordel, Quantification of fluorine traces in solid samples using CaF molecular emission bands in atmospheric air Laser-Induced Breakdown Spectroscopy, Spectrochim. Acta, Part B 123 (2016) 157–162.
[22] Z. Tang, R. Zhou, Z. Hao, W. Zhang, Q. Li, Q. Zeng, X. Li, X. Zeng, Y. Lu, Determination of fluorine in copper ore using laser-induced breakdown spectroscopy assisted by the SrF molecular emission band, J. Anal. At. Spectrom. 35 (2020) 754–761.
[23] D.S. Vogt, S. Schröder, K. Rammelkamp, P.B. Hansen, S. Kubitza, H.W. Hübers, CaCl and CaF emission in LIBS under simulated martian conditions, Icarus 335 (2020).
[24] Z. Tang, Z. Hao, R. Zhou, Q. Li, K. Liu, W. Zhang, J. Yan, K. Wei, X. Li, Sensitive analysis of fluorine and chlorine elements in water solution using laser-induced breakdown spectroscopy assisted with molecular synthesis, Talanta 224 (2021) 121784.
[25] M. Gaft, Y. Raichlin, F. Pelascini, G. Panzer, V. Motto Ros, Imaging rare-earth elements in minerals by laser-induced plasma spectroscopy: molecular emission and plasma-induced luminescence, Spectrochim. Acta, Part B 151 (2019) 12–19.
[26] D.M. Mattox, Physical sputtering and sputter deposition, in: D.M. Mattox (Ed.), Handbook of Physical Vapor Deposition (PVD) Processing, Elsevier, 2010.
[27] S.J.B. Reed, Sample Preparation, Electron Microprobe Analysis and Scanning Electron Microscopy in Geology, Cambridge University Press, 2005, pp. 149–161.
[28] Y. Dong, B. Li, S. Malitsky, I. Rogachev, A. Aharoni, F. Kaftan, A. Svatos, P. Franceschi, Sample preparation for mass spectrometry imaging of plant tissues: a review, Front. Plant Sci. 7 (2016) 60.
[29] Z. Gajarska, L. Brunnbauer, H. Lohninger, A. Limbeck, Identification of 20 polymer types by means of laser-induced breakdown spectroscopy (LIBS) and chemometrics, Anal. Bioanal. Chem. 413 (2021) 6581–6594.
[30] J.D. Hunter, Matplotlib: a 2D graphics environment, Comput. Sci. Eng. 9 (2007) 90–95.
[31] C.R. Harris, K.J. Millman, S.J. van der Walt, R. Gommers, P. Virtanen, D. Cournapeau, E. Wieser, J. Taylor, S. Berg, N.J. Smith, R. Kern, M. Picus, S. Hoyer, M.H. van Kerkwijk, M. Brett, A. Haldane, J.F. Del Rio, M. Wiebe, P. Peterson, P. Gerard-Marchant, K. Sheppard, T. Reddy, W. Weckesser, H. Abbasi, C. Gohlke, T.E. Oliphant, Array programming with NumPy, Nature 585 (2020) 357–362.
[32] P. Virtanen, R. Gommers, T.E. Oliphant, M. Haberland, T. Reddy, D. Cournapeau, E. Burovski, P. Peterson, W. Weckesser, J. Bright, S.J. van der Walt, M. Brett, J. Wilson, K.J. Millman, N. Mayorov, A.R.J. Nelson, E. Jones, R. Kern, E. Larson, C.J. Carey, I. Polat, Y. Feng, E.W. Moore, J. VanderPlas, D. Laxalde, J. Perktold, R. Cimrman, I. Henriksen, E.A. Quintero, C.R. Harris, A.M. Archibald, A.H. Ribeiro, F. Pedregosa, P. van Mulbregt, C. SciPy, SciPy 1.0: fundamental algorithms for scientific computing in Python, Nat. Methods 17 (2020) 261–272.
[33] G. Herzberg, Molecular Spectra and Molecular Structure-Vol I, Read Books Ltd, 2013.
[34] A. Limbeck, L. Brunnbauer, H. Lohninger, P. Porizka, P. Modlitbova, J. Kaiser, P. Janovszky, A. Keri, G. Galbacs, Methodology and applications of elemental mapping by laser induced breakdown spectroscopy, Anal. Chim. Acta 1147 (2021) 72–98.
[35] L. Brunnbauer, S. Larisegger, H. Lohninger, M. Nelhiebel, A. Limbeck, Spatially resolved polymer classification using laser induced breakdown spectroscopy (LIBS) and multivariate statistics, Talanta 209 (2020) 120572.
[36] R.A. Fisher, The use OF multiple measurements IN taxonomic problems, Annals of Eugenics 7 (1936) 179–188.
[37] K. Fukunaga, Introduction to Statistical Pattern Recognition, Elsevier, 2013.
[38] W.J. Youden, Index for rating diagnostic tests, Cancer 3 (1950) 32–35.